FABRICATION AND TESTING OF A MEMS BASED EARTH SENSOR

K. Ghose[*] and H.R. Shea
Ecole Polytechnique Fédérale de Lausanne (EPFL), Microsystems for Space Technologies Laboratory, Neuchâtel, Switzerland

ABSTRACT

We present a novel MEMS inertial sensor that directly measures the gravity gradient in order to sense the relative orientation of a satellite with respect to the Earth. An Earth sensor provides an orbiting satellite with a vector towards the Earth center. Current Earth sensors use optical methods to determine the Earth vector by sensing the IR emission from the Earth. This requires optical access on multiple faces of the satellite. We present here the microfabrication and preliminary testing of a much lighter and more compact MEMS-based approach to determine the Earth vector by measuring the torque induced on an elongated body due to the gravity gradient.

KEYWORDS

Earth sensor, gravity gradient torque, inertial sensor.

DESIGN OF THE EARTH SENSOR

Gravity Gradient Torque (GGT)

The gravitational force decreases as the inverse square of the distance to the Earth center. Different parts of an object orbiting the Earth are at slightly different distances from the earth's center, and therefore subject to minute differences in the gravitational force exerted on them. This results in a net torque around the axis of maximum moment of inertia. For orbiting satellites, this difference in gravity is small, but it has been used to stabilize the orientation of several small satellites with respect to the Earth. The satellite, generally equipped with a mass at the end of a boom, ends up with its axis of minimum moment of inertia pointing normal to the Earth's surface. The gravity gradient torque (GGT) is used here for the first time as the sensing scheme for an Earth sensor.

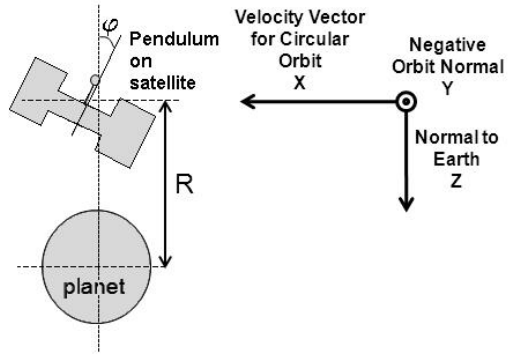

Figure 1: Reference axes and orientation for body in orbit for gravity gradient torque calculation.

Due to gravity gradient torque (GGT), a suitably shaped pendulum within a satellite will move relative to the rest of the satellite, depending of the orientation of the satellite with respect to the normal to the Earth. By sensing the movement of this pendulum the Earth vector can be computed. The expression for the GGT is given by [1]:

$$GGT = 3\mu \cdot |I_y - I_x|. \sin(2\varphi) / 2R^3_{orbit} \qquad (1)$$

where μ is the Earth's gravity constant and φ the angle to the Earth normal as seen in Figure 1, I_y and I_x are the moments of inertia of the suspended pendulum mass calculated about the negative orbit normal and velocity vector. To obtain greater GGT, a large moment of inertia is desirable, and the mass must be shaped to maximize I_x relative to I_y. A very compliant spring is desirable to obtain a larger displacement for a given GGT. As seen in Equation 1, due to the 2φ dependency, two pendulums, placed at an orientation of 45° to each other in one plane, are required to determine an angle of the Earth vector. For complete 4π sensing of the Earth vector, two such sets of pendulums are needed, placed at 90° relative to each other.

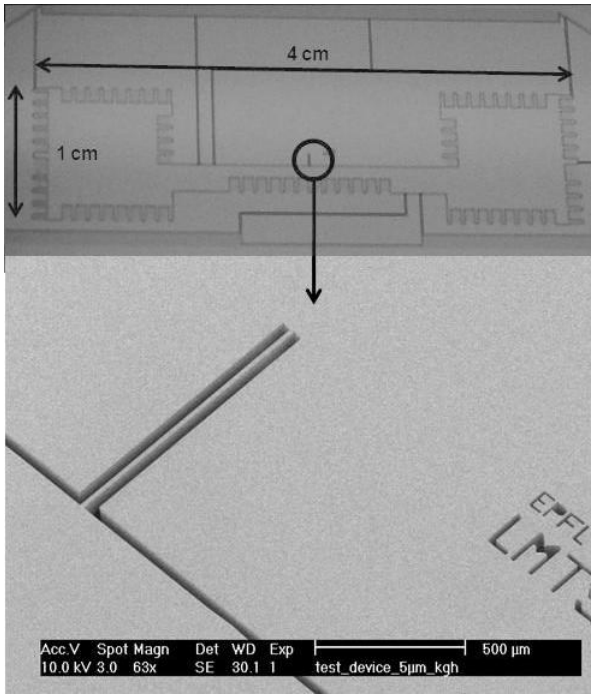

Figure 2: Top: Optical micrograph of the deep reactive ion etched silicon pendulum mass. Bottom: SEM image of the 1mm long, 15 µm wide, and 100 µm deep spring etched into the device layer of the SOI wafer.

In micro-gravity a large mass and compliant spring results in improved performance. Increasing the mass and hence I_y, or using a more compliant spring produce a greater displacement increasing the signal to thermal noise ratio [2]. However a larger mass suspended by a softer spring results in more fragile devices. The sensor is fabricated and tested in a one gravity environment. Making it robust enough to be handled and tested on Earth is the biggest challenge that we had to solve. Being able to obtain enough sensors per 4" wafer is also a limitation on the size of the mass. Accordingly, we use a 600 µm thick silicon pendulum of area 1×4 cm^2, suspended from a 1 mm long, 15 µm wide, 100 µm deep spring (see photo and SEM in Figure 2). The mass is shaped to maximize its moment of inertia I_y.

The dimensions of the spring are chosen so that it is very compliant for a torque around the Y axis (Figure 3) but very stiff when under one gravity along the Y axis, such as when the sensor is tested on Earth. The sensor mass is distributed in order to minimize the sag of the device when placed flat for testing.

Table 1 summarizes the device key dimensions and predicted displacement, which is of the order of nm for an orbital altitude of 300 km.

Table 1 Parameters of sensor mass and spring

Moment of Inertia (I_x-I_y)[kg.m^2]	6.70939×10^{-8}
Weight [g]	0.33
Spring constant	5.0625×10^{-6}
Peak GGT [N.m]	1.35×10^{-13}
Peak angular rotation [°]	1.52931×10^{-6}
Peak Displacement [nm]	0.534

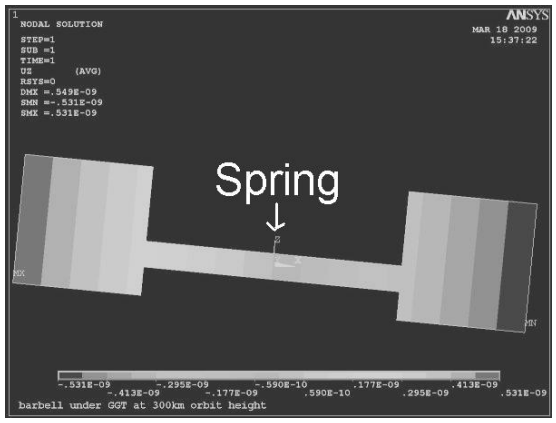

Figure 3: FEM simulation of pendulum under GGT, assuming an orbit of 300km.

Our first focus was developing a reliable fabrication process for this sensor, so we chose a 15 µm spring width. Since the fabrication process is validated, the next iteration of this sensor will have a 5 µm thick spring, and the displacement will be in the 10 nm range.

SENSOR FABRICATION

The motion of the sensor mass has to be limited so that the mass does not break off under routine handling. The major challenge we solved was developing a process flow that limits the motion of the 1×4 cm^2 proof mass to a few microns on all 3 axes, prior to it being released from the device frame, to make the device robust enough for testing on Earth.

The sensors are fabricated on 4" SOI wafers, which have a device layer thickness of 100 µm, oxide 1 µm and handle layer thickness of 500 µm. The pendulum is etched from both the device and handle layers since its mass, and therefore moment of inertia, has to be maximized. The Si MEMS pendulum has a mass of 0.33 g, and its top outline dimensions are 1×4 cm^2. The first step is to define the mass shape and chip outline by DRIE of the handle layer.

The next step is DRIE of the device layer to define the mass shape in the device layer and etch the spring. Stoppers are etched into the device layer to restrict the motion of the mass in the X-Z plane to 30 µm. (Figure 4). Parts of the device layer are made to overlap with the handle layer, keeping the sensor mass attached to the chip by means of the oxide.

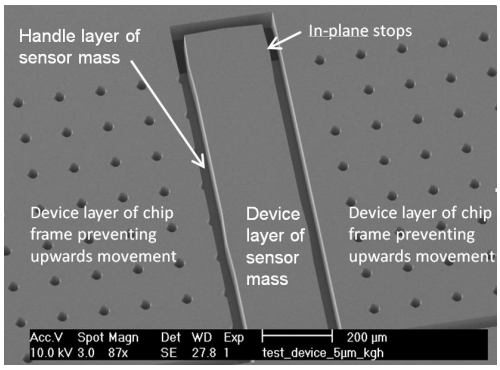

Figure 4: SEM image of stops to constrain sensor mass from excessive movement due to handling or satellite re-orientation (max motion in plane: 30 µm X and Y, max motion out of plane: 1.5 µm up, 30 µm down).

Using HF vapor, the SOI chips, each with one pendulum, are first released from the SOI wafer. At this point, the sensor mass is still attached by oxide to the chip frame. A Pyrex chip, patterned to contain an array of spikes giving 30 µm clearance to the sensor mass (Figure 5), is bonded to the SOI handle layer of the chip frame. The sensor mass is finally released in HF vapor. The mass is constrained from moving downwards by the Pyrex wafer, a similar approach to what was reported in [3]. It is prevented from moving upwards by having the chip's device layer overhang the pendulum. Thus the mass is constrained to 30µm of motion prior to release. A successfully completed device is shown in Figure 7.

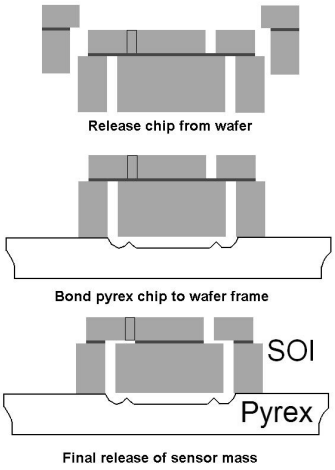

Figure 5: Schematic of the last assembly steps. To prevent the spring from breaking during fabrication, the proof mass is only released in HF vapor after the SOI chip is bonded to an etched Pyrex wafer.

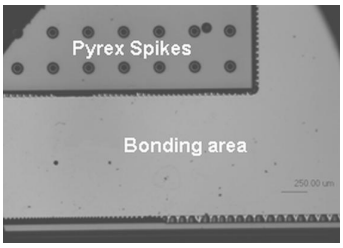

Figure 6: Optical micrograph top view of fabricated Pyrex chip showing the bonding area and spikes to limit sensor mass motion.

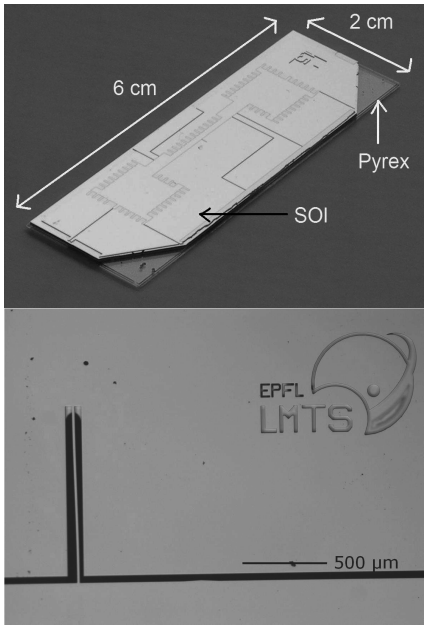

Figure 7: Top: Photograph of the fabricated Earth sensor. Bottom: optical micrograph of the released spring.

OPTICAL DISPLACEMENT READOUT

The pendulum displacement is measured with an integrated fiber-based interferometer, similar in concept to [4]. We first fabricated a test chip consisting of a movable mass suspended by eight springs, identical to those on the final device. An optical fiber was integrated into the test chip (Figure 8). The mass was moved relative to the fiber tip and the resulting intensity at the measuring photodiode was recorded (Figure 9), confirming the fiber based interferometer is suitable for measuring displacements in the 10 nm range.

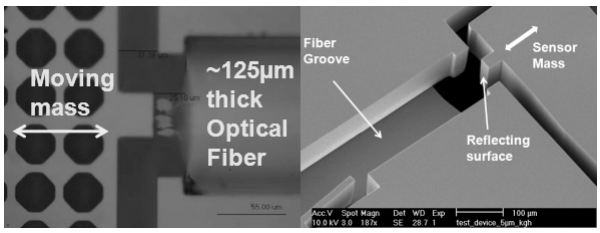

Figure 8: Left: Top view of fiber interferometer integrated onto a test chip with 635 nm laser light exiting and being reflected back into single-mode fiber. Right: SEM image of fiber mounting and interferometer geometry on a fabricated MEMS Earth sensor.

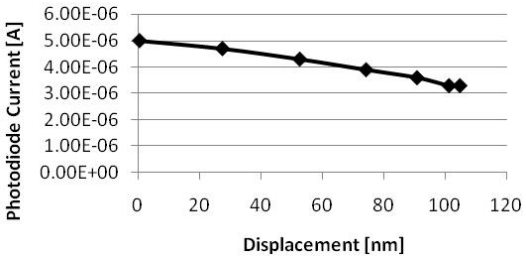

Figure 9: Interferogram obtained from test chip by measuring current at photodiode while changing the distance between the reflecting silicon surface and fiber tip.

TESTING THE EARTH SENSOR

The Earth sensor is designed to measure gravity gradient torques in a microgravity environment. We simulate the torque in the lab by applying very small tilts to the device. We mount the sensor on a piezo driven tip-tilt stage capable of arc second resolution. By tilting the sensor by a few arcseconds, the mass moves by a few nanometers relative to the fiber tip, and we record the resulting intensity change at the measuring photodiodes (see figure 10)

Since the piezos are driven in open loop mode, we placed a position sensitive detector (PSD) at a fixed distance from the sensor. It detected a laser beam reflecting from the polished silicon surface of the sensor frame. As the piezo tip-tilt stage was moved, the distance traversed by the reflected laser spot was recorded on the PSD. From this the angle through which the piezo moved was calculated to be 0.0142°. Although the tip tilt stage is

capable of a total of 0.0333° of travel, we limited the movement to 0.0142° to avoid having the mass bump a stopper, since the device is designed to give the mass only 1.5 µm upwards clearance and because we are trying to detect motion in the 10 nm range, which should be achieved for this reduced tilt angle.

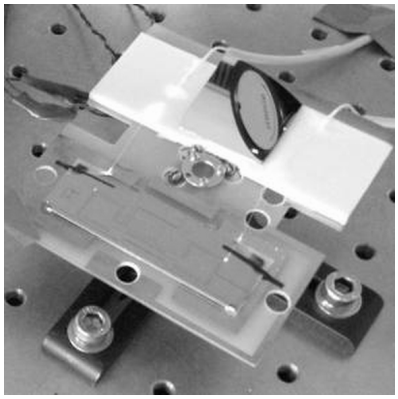

Figure 10: Earth sensor on piezo tip-tilt stage

We performed FEM simulations to determine the displacement of the sensor mass when the device is rotated over this range. From simulation it is determined that the mass moves by 21 nm relative to the fiber tip (Figure 11).

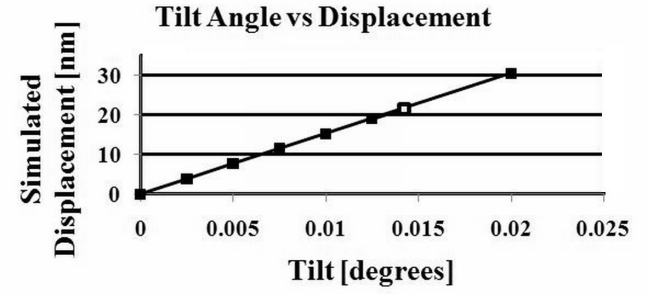

Figure 11: Simulated displacement of sensor mass relative to fiber tip with changing tilt angle of piezo tip-tilt stage

RESULTS

Fiber based interferometers are integrated into the sensor (Figure 8) and used to monitor the displacement of the sensor mass. Figure 12 shows the change in photocurrent as increasing voltages are applied to the piezo, thus tilting the sensor from 0 to 0.0142°.

Some noise is seen in the photocurrent measurement since we are at the limit of the measuring ammeter. Since the current is measured for a 42 nm change in optical path length, and the laser used in the fiber interferometer has a wavelength of 635 nm, a very small section of the interferogram is seen. This prevents us from making a precise conversion from photocurrent to displacement.

Comparing figure 8 with figure 11, one can see that the device operates as expected, moving by nm in response to a tilt that simulated the torque that would be experienced due to the gravity gradient.

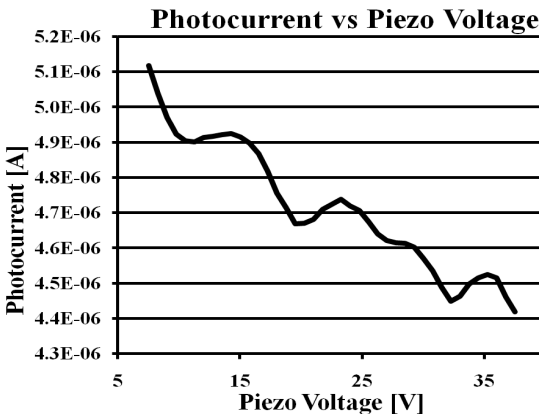

Figure 12: Photocurrent at measuring photodiode, of the fiber interferometer of earth sensor as voltage applied to the tip-tilt piezo increases, changing the tilt angle by 0.0142°

CONCLUSION

We were able to successfully fabricate and test in a one gravity environment a sensor meant for use in microgravity. We duplicated the expected range of motion in microgravity using a tip-tilt stage and measured the displacement using an integrated fiber based interferometer. As seen from Figures 11 and 12 the measurement of the photocurrent shows an appreciable change with changing distance between the sensor mass and the fiber tip in the 10 nm range. The fabrication process is well established and the next iteration of devices will have 5 µm wide springs instead of the current 15 µm. The photocurrent was measured directly. By using improved techniques such as closed loop operation and lock-in methods we have room to considerably improve the displacement readout.

REFERENCES

[1] J.R. Wertz, W.J. Larson, *Space Mission Analysis and Design*, Kluwer Academic Publishers, Dordrecht, 1999

[2] T.B. Gabrielson, "Mechanical-Thermal Noise in Micromachined Acoustic and Vibration Sensors", *IEEE Transactions on Electron Devices*, Vol. 40, pp. 903-909, 1993

[3] T.P.Swiler, U. Krishnamoorthy, P.J. Lewis, M.S. Baker, D.M. Tanner, "Challenges of designing and processing extreme low-G microelectromechanical system (MEMS) accelerometers", in *Reliability, Packaging, Testing, and Characterization of MEMS/MOEMS VII Conference*, San Jose, January 21, 2008, 68840O

[4] D. Rugar, H.J. Mamin, P. Guethner, "Improved fiber-optic interferometer for atomic force spectroscopy", *Appl. Phys. Lett.*, Vol. 55, pp. 2588-2590, 1989

CONTACT

*K. Ghose, tel: +41-32-720-5166; kaustav.ghose@epfl.ch